

Strengthening mechanism by Ti-N clusters and nano-sized TiN precipitate formed during nitriding of Fe-Ti alloy

Goro Miyamoto¹, Kyoka Itasaka², Tadashi Furuhashi¹

¹ Institute for Materials Research, Tohoku University, 2-1-1 Katahira, Aoba-ku, Sendai, Miyagi, 980-8577 Japan.

² Formerly graduate student Department of Metallurgy, Tohoku University, 2-1-1 Katahira, Aoba-ku, Sendai, Miyagi, 980-8577 Japan (now at Honda Motor Co.)

Nano-precipitates or nano clusters are known to lead the surface hardening of alloyed steels in nitriding treatment while strengthening behavior concerning the distribution of clusters and nano-sized precipitates is unclear. Therefore, this study aims to quantify the distribution of clusters and nano-sized alloy precipitates in Fe-Ti alloys nitrided and followed by denitrided to remove N in solution and clarify the interaction of those precipitates against dislocation. Clusters are formed at low nitriding temperature while coarser TiN precipitates become dominant at higher nitriding temperatures. Based on the size and volume fraction of precipitates, average inter-particle spacing (L) on the slip plane is evaluated. L first decreases with an increase in nitriding temperature from 550 to 650 °C, then increases at 700 °C. Temperature dependence of precipitation strengthening is consistent with that of L . The interaction force between precipitate and dislocation is much lower than that predicted by the Orowan mechanism and increases with an increase in the thickness of precipitates. Such size dependency of the interaction force suggests cutting mechanism is responsible for the hardening in nitriding of Fe-Ti alloys.

Keywords: nitriding, strengthening mechanism, nano-precipitates

1. Introduction

Nitriding is a popular surface hardening treatment for steels to improve fatigue strength and wear properties. It is well known that nano-sized alloy nitrides or solute clusters consisting of nitrogen (N) and substitutional element (s) are responsible for surface hardening in nitriding of steels bearing with nitriding forming elements such as Ti, V, Al, and Cr, etc.^{1,2}. The strengthening mechanism of nano-precipitates in steels has attracted much attention, and the relation between nano TiC distributions and amount of strengthening was investigated³, or deformation of VC after tensile deformation was directly investigated⁴. In those studies, the amount of strengthening is decreased at smaller precipitate size³ unlikely to Orowan mechanism or precipitate is sheared after tensile deformation⁴. Accordingly, nano-sized alloy carbides could contribute strength by the cutting mechanism. On the other hand, the strengthening mechanism of nano-sized alloy nitrides or N-s clusters has not been well investigated.

Therefore, this study aims to quantitatively compare the distribution of clusters and nano-sized alloy nitrides with the strength to clarify the interaction of those precipitates against dislocation motion⁵.

2. Experimental procedure

Ti is selected to form N-s cluster⁶, and thin plate (about 0.8 mm thick) of Fe-0.1Ti specimens with equiaxed ferrite (α) structure was gaseous-nitrided uniformly up to center region at 550-700 °C for 12 h at nitriding potentials in α the region as shown in Lehrer diagram of Fig. 1. The nitrided specimens are subsequently hydrogen-annealed at 480 °C for 60 h to remove N in solution, which will be referred to as denitriding treatment. The N content was quantified by weight change after the nitriding and denitriding treatment and shown in Fig. 2. The concentration of N after nitriding treatment increases at lower nitriding temperature and

decreases up to nearly equal to the nominal Ti concentration after the denitriding treatment regardless of nitriding temperature. Thus, all the Ti atoms should be present in forms of Ti-N clusters or TiN precipitates after denitriding treatment. Mechanical properties were evaluated using Vickers hardness measurement and tensile tests. Nano precipitates were characterized using scanning transmission electron microscopy (STEM) and a three-dimensional atom probe (3DAP).

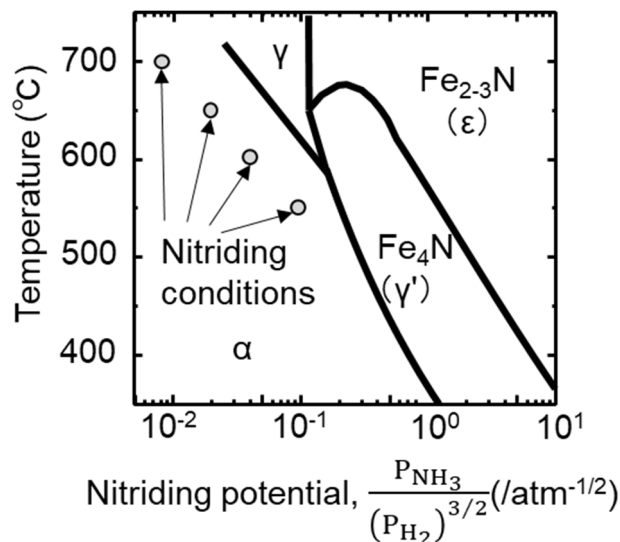


Fig. 1 Lehrer diagram showing the nitriding conditions used in the present study.

3. Results and discussions

Fig. 3 shows variations in the Vicker hardness of the nitrided and denitrided specimens as a function of nitriding temperature. The hardness of the specimen increases by nitriding and becomes lower at higher nitriding temperatures.

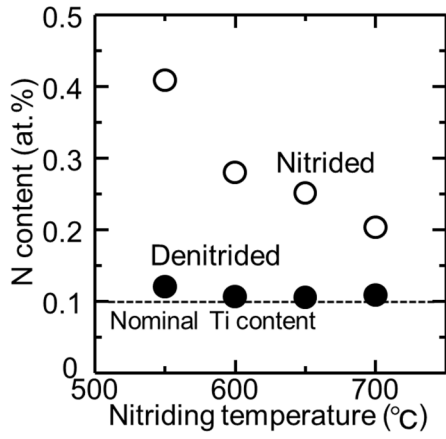


Fig. 2 N contents of nitrided and denitrided specimens as a function of nitriding temperature.

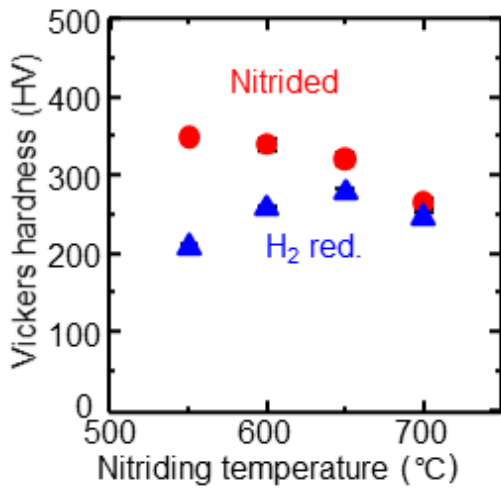


Fig. 3 Vickers hardness of nitrided and denitrided specimens as a function of nitriding temperature.

Subsequent denitriding results in softening, and degree of softening is smaller at higher temperatures. As a result, the maximum hardness is achieved at 650 °C after the denitriding treatment.

Fig. 4 shows stress-strain curves of the Fe-0.1Ti alloys nitrided and denitrided compared to the unnitrided specimen. The yield strength (Y_s) and ultimate tensile strength both increase by nitriding and denitriding. Y_s increases with an increase in nitriding temperature up to 650 °C while it drops at 700 °C. Elongation is reduced significantly by nitriding and denitriding treatments compared to an unnitrided specimen. The uniform elongation tends to decrease at higher nitriding temperatures.

Nano-structures in the specimens nitrided at 600, 650, and 700 °C followed by denitriding treatment were shown in Figs 5(a)-(c), respectively. Disk-shaped precipitates are formed along $\{001\}_\alpha$ in all the specimens. When the nitriding temperature is low, most precipitates are Ti-N clusters whose thickness is less than three atomic layers (Fig. 5(a)). Meanwhile, rising nitriding temperature leads to the formation of coarser TiN precipitates (Figs. 5(b), (c)).

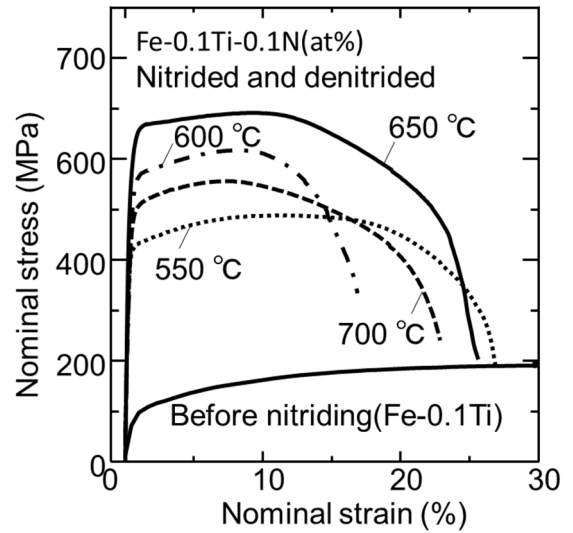


Fig. 4 Stress-strain curves of Fe-0.1Ti alloys nitrided at various temperatures followed by denitrided. Stress-strain curve of the Fe-0.1Ti alloy before nitriding is also shown as a comparison.

Based on the size and volume fraction of precipitates, average inter-particle spacing (L) on the slip plane is evaluated (Fig. 5(d)). L first decreases with an increase in nitriding temperature from 550 to 650 °C, then increases at 700 °C. Temperature dependence of precipitation strengthening (σ_{ppt}) shown in Fig. 5(e) is consistent with that of L . It was found that the highest strength at 650 °C is resulted from the highest precipitate number density on the slip plane.

The interaction force between precipitates and dislocation (F) can be evaluated from eq. 1

$$F = \frac{Lb\sigma_{ppt}}{0.8M} \quad \text{eq. 1}$$

where b and M are Burgers vector and Taylor factor (2.8), respectively. The estimated F ranges 1-2 nN, which is much smaller than the interaction force predicted by the Orowan mechanism, namely, $F_{Orowan} = Gb^2 \cong 5.0$ nN. These results imply that TiN or Ti-N clusters formed in the nitriding treatment contribute to strength via the cutting mechanism.

4. Summary

The microstructure and strength of the Fe-0.1Ti alloy nitrided at various temperatures and denitrided at lower temperatures were investigated. The maximum strength is achieved in nitriding at 650 °C followed by denitriding. Ti-N clusters are dominantly formed at 600 °C, while coarse TiN precipitation occurs at higher nitriding temperatures. The interparticle spacing of precipitates on the slip plane becomes minimum in nitriding at 650 °C, and its temperature variation is consistent with precipitation strengthening. The much smaller interaction force between dislocation and precipitates than the Orowan mechanism prediction suggests that the cutting mechanism occurs in the strengthening by TiN and Ti-N clusters in this study.

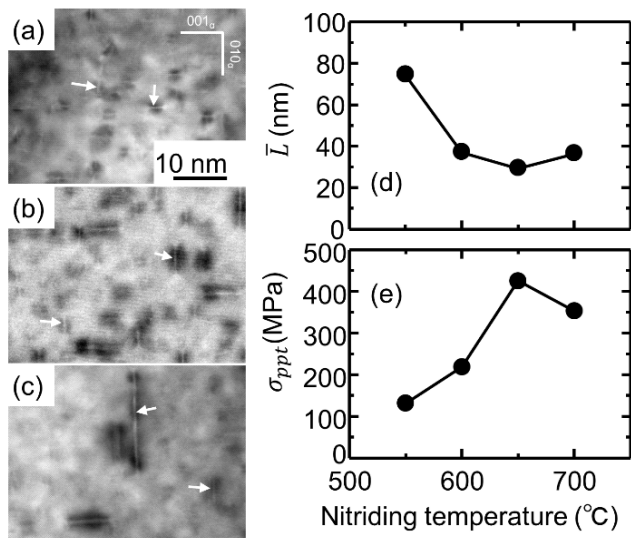


Fig. 5 (a), (b), (c) STEM-annular bright field images taken from the specimens nitrided at 600, 650 and 700 °C, respectively, followed by denitriding, (d), (e) variations of \bar{L} and σ_{ppt} with temperature.

References

- 1) E. J. Mittemeijer and M. A. J. Somers: *Thermo-chemical Surface Engineering of Steels*, Elsevier, (2015).
- 2) G. Miyamoto, Y. Tomio, H. Aota, K. Oh-ishi, K. Hono and T. Furuhashi: *Mater. Sci. Technol.*, **27**(2011), 742-746.
- 3) Y. Kobayashi, J. Takahashi and K. Kawakami: *Scripta Mater.*, **67** (2012), 854-857
- 4) E. Pereloma, D. Cortie, N. Singh, G. Casillas and F. Niessen: *Mater. Res. Lett.*, **8**(2020), 341-347.
- 5) K. Itasaka, G. Miyamoto, T. Furuhashi: *CAMP-ISIJ*, **33**(2020), 587.
- 6) D. S. Rickerby, S. Henderson, A. Hendry and K. H. Jack: *Acta Metall.*, **34**(1986), 1687-1699.

Acknowledgements

This work was supported by the JST Collaborative Research Based on Industrial Demand (Grant No. JPMJSK1613, Japan), JST FOREST Program (Grant No. JPMJFR203W, Japan), MEXT Program Data Creation and Utilization Type Material Research and Development Project (Grant Number JPMXP1122684766). T.F. and G.M. gratefully acknowledge the support provided by the MEXT through Grants-in-Aid for Scientific Research (A) (No. 17H01330, 2017–2019), Grant-in-Aid for Scientific Research (B) (No. 19H02473, 2019–2021), Grant-in-Aid for Scientific Research on Innovative Areas (Research in a proposed research area) (No. 18H05456, 2018–2022), Grant-in-Aid for Challenging Research (Exploratory)(No. 21K18803, 2021–2022). The Tohoku University Microstructural Characterization Platform in Nanotechnology Platform Project, sponsored by the Ministry of Education, Culture, Sports, Science and Technology (MEXT), Japan is also acknowledged.